NANOMATERIALS

Locking volatile organic molecules by subnanometer inorganic nanowire-based organogels

Simin Zhang[1], Wenxiong Shi[2], Xun Wang[1]*

The intermolecular forces among volatile organic molecules are usually weaker than water, making them more difficult to absorb. We prepared alkaline earth cations–bridged polyoxometalate nanoclusters subnanometer nanowires through a facile room-temperature reaction. The nanowires can form three-dimensional networks, trapping more than 10 kinds of volatile organic liquids effectively with the mass fraction of nanowires as low as 0.53%. A series of freestanding, elastic, and stable organogels were obtained. We prepared gels that encapsulate organic liquids at the kilogram scale. Through removing solvents in gels by means of distillation and centrifugation, the nanowires can be recycled more than 10 times. This method could be applied to the effective trapping and recovery of organic liquids.

Water-based hydrogels can be easily prepared through the formation of hydrogen bond networks between water molecules and gelators such as polymer chains and/or inorganic nanostructures (*1*–*3*). Compared with hydrogen bonds, the intermolecular forces among volatile organic molecules are usually weaker, hindering the semisolidification of volatile organic liquids and development of functional organogel materials.

Subnanometer nanowires (*4*–*7*) can form three-dimensional (3D) networks and gels similar to polymers. We prepared alkaline earth metal cations–bridged polyoxometalate nanoclusters (AE-POM) subnanometer nanowires through a facile room-temperature reaction [supplementary materials (SM), materials and methods 1.2].

First, we prepared calcium-POM (Ca-POM) nanowires. We investigated morphologies of Ca-POM nanowires through transmission electron microscopy (TEM), atomic-resolution aberration-corrected TEM (AC-TEM), atomic force microscopy (AFM), and small-angle x-ray diffraction (SXRD). The nanowires dispersed in octane with a length of several micrometers and were curved and entangled with each other (Fig. 1, A and B, and fig. S1). The diameter could be distinguished from AFM data, which was ~1 nm (Fig. 1, C and D), so the aspect ratio was as high as several thousands. The spacing distance between two nanowires was calculated from the SXRD data as ~3.78 nm (fig. S2). As shown in the atomic-resolution AC high-angle annular-dark field

[1]Laboratory of Organic Optoelectronics and Molecular Engineering, Department of Chemistry, Tsinghua University, Beijing 100084, China. [2]Institute for New Energy Materials and Low Carbon Technologies, School of Materials Science and Engineering, Tianjin University of Technology, Tianjin 300387, China.
*Corresponding author. Email: wangxun@mail.tsinghua.edu.cn

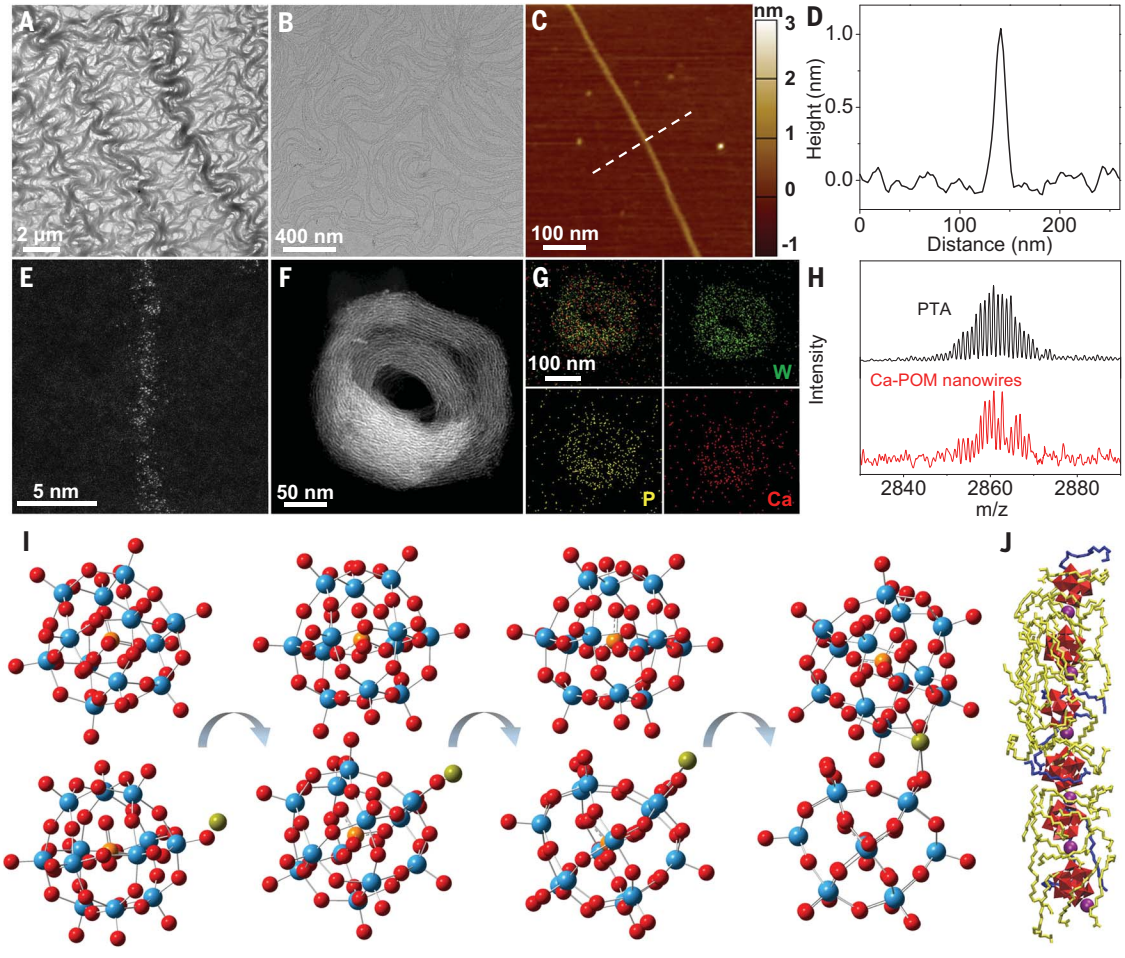

Fig. 1. Morphologies of Ca-POM nanowires. (**A** and **B**) TEM images of nanowires. (**C**) Typical AFM topographic image of the nanowire and (**D**) the line profile along the dashed line. (**E**) AC-HAADF-STEM image of the nanowire. (**F**) STEM image and (**G**) corresponding EDS elemental mapping images of coiled nanowires. (**H**) MALDI-TOF-MS results of PTA and nanowires. (**I**) Geometry optimization of nanowires structure. The red, blue, orange, and yellow balls indicate O, W, P, and Ca, respectively. (**J**) The structural diagram of the nanowire. Purple balls indicate Ca^{2+}, red models indicate $PW_{12}O_{40}^{3-}$ nanoclusters, and yellow and blue chains represent oleylamine and protonated oleylamine, respectively.

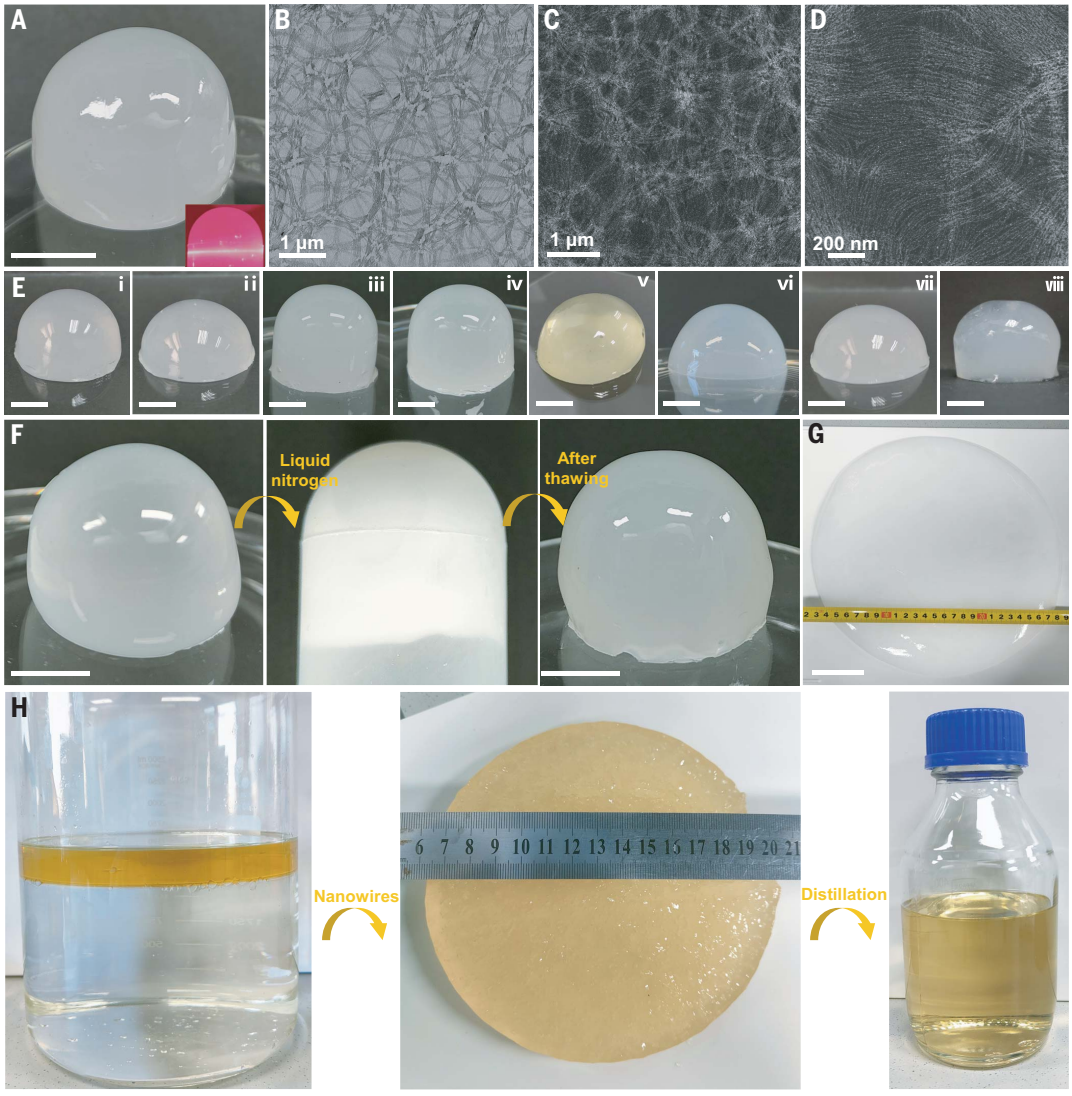

Fig. 2. Ca-POM nanowire–organic liquids gels. (**A**) Photograph of the nanowires-octane gel. (Inset) The Tyndall effect of the gel. (**B**) TEM image and (**C** and **D**) STEM images of nanowire networks. (**E**) Photographs of nanowire-organic liquids gels: (i) cyclohexane, (ii) hexane, (iii) toluene, (iv) 2,5-dimethyl-2,5-di-(tert-butylperoxy) hexane, (v) petrol, (vi) n-propyl ether, (vii) 1-dodecanethiol, and (viii) octadecene. (**F**) Photographs of a nanowire-octane gel frozen in liquid nitrogen and subsequently thawed. The gel was sealed in a tube and then placed in liquid nitrogen. (**G**) A nanowire-octane gel with a diameter of ~26 cm and thickness of ~1.5 cm. (**H**) Photographs of oil spill recovery process with nanowires. The nanowire-petrol gel has a diameter of ~15 cm and thickness of ~2 cm. Scale bars, (A), (E), and (F) 1 cm; (G) 5 cm.

scanning TEM (AC-HAADF-STEM) image (Fig. 1E), the nanowire was mainly composed of nanoclusters. When ethanol was added into the dispersion of nanowires in octane, the nanowires coiled, and some nanorings formed (Fig. 1F and fig. S3), demonstrating their high flexibility. The composition of nanowires was investigated through x-ray photoelectron spectroscopy (XPS) and energy dispersive x-ray spectroscopy (EDS) elemental mapping. Ca-POM nanowires were mainly composed of Ca, tungsten (W), phosphorus (P), and oxygen (O) (fig. S4). The EDS mapping demonstrated that Ca, W, and P dispersed in nanowires uniformly (Fig. 1G). The structure of nanowires was further investigated through Fourier transform infrared (FTIR) spectroscopy and matrix-assisted laser desorption ionization time-of-flight mass spectrometry (MALDI-TOF-MS). As shown in fig. S5, the FTIR characteristic absorption peaks of phosphotungstic acid (PTA) also appeared in the FTIR spectrum of nanowires (*8*), suggesting that $PW_{12}O_{40}^{3-}$ nanoclusters existed in nanowires. The absorption peaks at 2850 and 2915 cm^{-1} belonged to oleylamine. We further used MALDI-TOF-MS to test PTA and nanowires, revealing the existence of $PW_{12}O_{40}^{3-}$ in nanowires. Because PTA and Ca-POM nanowires were broken into $PW_{12}O_{39}^{-}$ fragments during the ionization process, the peak positions shifted to about 2860 (Fig. 1H and fig. S6) (*9*). The pK_a (–log10K_a, where K_a is the acid dissociation constant) of protonated oleylamine is 10.7, and the pK_a3 of PTA is 2.0 to 3.3 (*10*, *11*). During the experiment, ~0.347 mmol PTA and 9.7 mmol oleylamine were added, so PTA was completely dissociated as H^+ and $PW_{12}O_{40}^{3-}$, and oleylamine was protonated, which was also demonstrated by the FTIR spectra (fig. S7). According to the inductively coupled plasma-atomic emission spectrometry (ICP-AES) data (table S1), the ratio of $PW_{12}O_{40}^{3-}$ to Ca^{2+} in nanowires was about 1:1, so there should be protonated oleylamine with equal molar quantity of $PW_{12}O_{40}^{3-}$ on nanowires to maintain electrical neutrality. Molecular dynamics (MD) simulations (movie S1) and geometry optimization (Fig. 1I and fig. S8) demonstrated that the Ca^{2+} bridged $PW_{12}O_{40}^{3-}$ in the final stable state of nanowires. According to the above characterization results, Ca^{2+} bridged $PW_{12}O_{40}^{3-}$ nanoclusters through electrostatic interaction to form nanowires, and oleylamine and protonated oleylamine attached to nanowires through coordination and electrostatic interactions (Fig. 1J). MD simulations were also run to investigate the formation of coiled nanowires (movie S2 and fig. S9), demonstrating that a decrease of surface energy drives the coiling process.

We prepared strontium-POM (Sr-POM) nanowires through the same method (fig. S10), and the structures were similar to that of Ca-POM nanowires (fig. S11 and table S1). We also tried many other metal cations and POMs; however, no nanowires were obtained when Ca^{2+}/Sr^{2+} or PTA was replaced (SM materials and methods 1.5 and figs. S12 to S16). The concentration,

solvent, and properties of counterions and POM anions influence the coordination modes of counterions and POM anions and their collective states (*12*, *13*). The formation of nanowires requires not only the 1D coordination mode of counterions and POM anions but also the nucleation of building blocks of nanowires from the reaction system and their connection into stable nanowire structures. For other metal counterions and POM anions, they show different self-assembly behavior with Ca^{2+} or Sr^{2+} and PTA anions. The mixed solvents and surfactants used in this work also influence their coordination modes and assembly behavior. Thus, not all metal counterions and POM anions can be prepared into nanowires in this experimental condition. The ratio of $Ca(NO_3)_2$ to PTA added into the reaction also influenced the products (fig. S17). MD simulation results showed that when there was excessive $PW_{12}O_{40}^{3-}$, they would combine more protonated oleyamine, and the nanoclusters tend to be aggregate and form nanosheets (fig. S18A). When there was excessive Ca^{2+}, it would combine with oleylamine, and some nanoparticles formed (fig. S18B), which is consistent with experimental results.

Experimentally, we found that the nanowires dispersion readily formed a gel (SM materials and methods 1.4), and the Tyndall effect is shown in Fig. 2A, inset. Inversion of a test tube showed that the gel was stable, and after standing for several hours at room temperature, a freestanding gel could be obtained (Fig. 2A). The critical gel concentration (CGC) was 0.53%, denoting the minimum mass percent of nanowires necessary for gelation of organic liquids. As shown in Fig. 2, B and C, nanowires intersected with each other in junctions and formed 3D networks in the gel. As shown in Fig. 2D, nanowires outside junctions were parallel to each other and formed a layer. Interwoven nanowires and parallel nanowires formed the structure with many cavities, which could lock organic liquids. For wet gels, the existence of octane in the gel showed plump vesicles (fig. S19A), whereas the vesicles were shriveled after the gel was dried (fig. S19B), and the originally convex morphology changed to the concave morphology. We prepared various organogels with low CGCs (Fig. 2E, fig. S20, and table S2), demonstrating that nanowires were widely applicable gelators for organic liquids. Sr-POM nanowires could also be used to prepare organogels (fig. S21); however, for the same organic liquid, the CGC of Sr-POM nanowires was higher than that of Ca-POM nanowires (table S3) because of the higher relative atomic mass of Sr. Moreover, through removing solvents in gels by means of distillation and centrifugation, nanowires in gels could be recycled more than 10 times to prepare gels (SM materials and methods 1.7 and

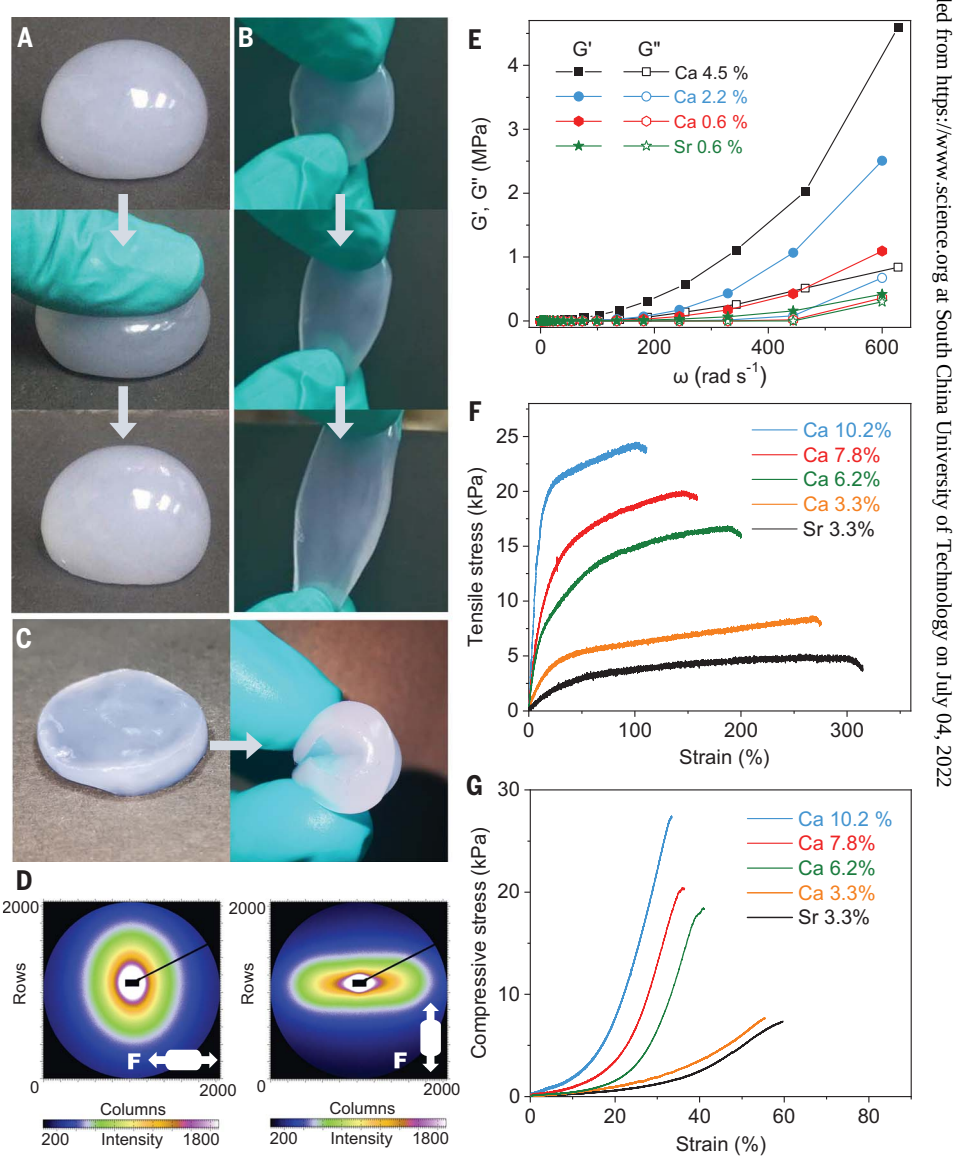

Fig. 3. Mechanical behaviors of nanowires-octane gels. (**A**) Photographs of the gel, which was compressed. (**B**) Photographs of the gel flake, which was stretched. (**C**) Photographs of the gel flake, which was folded. (**D**) SAXS 2D patterns of stretched gel flakes. Tensile directions are shown at bottom right. (**E**) Rheological study of gels in the frequency sweep mode for the strain amplitude of 1%. (**F** and **G**) Typical (F) tensile stress-strain curves and (G) compressive stress-strain curves of gels. Element symbols and numbers in the color keys in (E) to (G) indicate the type of nanowires and their mass percent in gels. For example, Ca 10.2% indicates Ca-POM nanowire-octane gels with 10.2% nanowires.

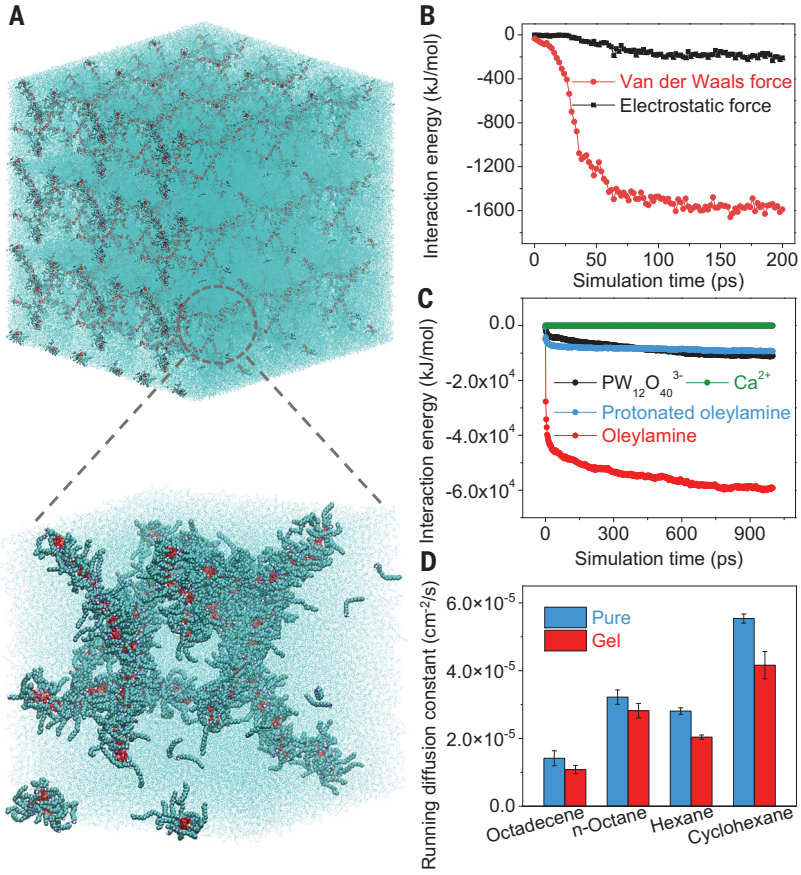

Fig. 4. MD simulations of Ca-POM nanowires-based gels. (**A**) Schematic diagram of the nanowire-octane gel. Small blue models indicate octane, and large blue-red models indicate nanowires. (**B**) The interaction energy between nanowires. (**C**) The interaction energies between octane and main parts of nanowires. (**D**) The running diffusion constants of some pure organic liquids and these liquids trapped in nanowire networks.

fig. S22). The purity of recovered organic liquids from gels was tested as higher than 99.5% (fig. S23), with a little ethanol impurity introduced during the washing process. Nanowires-based gels were stable, and no observable change occurred after 2 months of storage in sealed containers (fig. S24). The gel also remained stable after being frozen with liquid nitrogen (Fig. 2F). The production yield of nanowires could be increased through increasing the quantity of raw materials with equal proportion (SM materials and methods 1.3). As shown in Fig. 2G and fig. S25, gels with bigger sizes were obtained in two batches, with 603 and 373 g octane trapped, respectively. As shown in Fig. 2H, the spilled petrol (~330 ml) on water could form a gel with nanowires, and the freestanding nanowires-petrol gel could be overall removed from water. Then petrol could be separated from the gel through distillation (SM materials and methods 1.8).

The gel was elastic and flexible (Fig. 3, A to C). It could quickly return to its original shape after being compressed (movie S3), and when Ca-POM nanowires in the gel were ~60%, the gel could bounce (movie S4). When the size of gels greatly increased, its elasticity was maintained (movie S5). As shown in small-angle x-ray scattering (SAXS) results (Fig. 3D), when the gel flake was stretched, the SAXS 2D pattern was anisotropic, demonstrating that nanowires in the gel were oriented to a certain extent under tension.

As shown in Fig. 3E, storage modulus (G′) was higher than loss modulus (G″) for a gel, indicating that the gel exhibited more elastic property than viscosity. Because there is a 3D nanowire network in the gels, and because in the low angular velocity (ω) range G′ was higher than G″, there must be a physical cross-link in gels that results from entangling and interactions between nanowires. When nanowires in gels increased, G′ increased far more than G″, with a greater increase in the elasticity, because the density of cross-linked nanowire networks became higher. With ω increasing, nanowires in the gel were partly oriented under external force, so G′ increased rapidly. Sr is heavier than Ca, so there were fewer nanowires in the Sr-POM nanowires-octane gel than in the Ca-POM nanowires-octane gel with the same content of nanowires; thus, G′ of the gel with 0.6% Sr-POM nanowires was lower than the gel with 0.6% Ca-POM nanowires. As shown in Fig. 3F, the stress initially increased quickly and linearly with strain, mainly induced by elastic deformation of nanowire networks. After the yield point, nanowire networks gradually broke under tension, and deformation of gels was permanent. Last, a crack appeared on the gel that propagated under tension until the gel broke. As shown in Fig. 3G, the compressive stress initially increased slowly and linearly with the strain, mainly induced by elastic deformation of the nanowire networks. The stress subsequently increased faster with the strain, induced by permanent deformation of the nanowire networks. In this stage, the energy dissipation involved dissociation of the nanowire networks (*14*). Cracks on the gel gradually increased, causing the gel to be broken into several large pieces, rather than a catastrophic fracture into many small pieces. As shown in tables S4 and S5, when Ca-POM nanowires in gels increased from 3.3 to 10.2%, the tensile elastic modulus, tensile strength, compressive elastic modulus, and compressive fracture strength of the gels all increased, but the elongation at break and the compressive fracture strain decreased, which was also induced by the increase of density of the cross-linked nanowire networks. The octane content affected both the free volume and the lubricity among nanowires, so when the octane content was higher, deformability of gels was better (*15*). For the same gel, the tensile elastic modulus was higher than the compressive elastic modulus (tables S4 and S5). When the gel was stretched, nanowires were oriented to a certain extent under tension (Fig. 3D), and while the gel was compressed, there was no alignment of nanowires to resist compression. The mechanical properties of gels with 3.3% Ca-POM nanowires were better than that of gels with 3.3% Sr-POM nanowires, further demonstrating that the Ca-POM nanowires were better than Sr-POM nanowires as gelators. As shown in fig. S26, the strength of the gel improved when the standing time increased from 1 to 2 days, but further improvement was not apparent after 2 days. Nanowire-based gels were obtained through standing nanowire dispersions for several hours, achieving a preliminary stability of the nanowire networks. Through further standing, nanowire networks and trapped liquids achieved equilibrium. At this point, the gel was fully "mature" and did not evolve further (*16*). Organogels with previously reported high solvent content were usually not freestanding, and most of them did not perform tensile and compression tests. As shown in fig. S27, G′ of the nanowire-based gel was higher than most of the organogels with previously reported high solvents

content, demonstrating the good elasticity of the nanowire-based gel.

We used MD simulations to investigate Ca-POM nanowire-based gels. First, nine nanowires and 24,850 octane molecules were put into a closed system with the dimensions of 20 by 20 by 20 nm. After running MD simulations, nanowires formed networks driven by a decrease of potential energy (Fig. 4A). In addition to van der Waals forces, there were also electrostatic forces between nanowires (Fig. 4B), from the interaction between Ca^{2+} and $PW_{12}O_{40}^{3-}$ nanoclusters. The interactions between nanowires and octane, hexane, cyclohexane, and octadecene were strong, whereas the interactions between nanowires and chloroform were weak (fig. S28), so the nanowires dispersion in chloroform could not form a freestanding gel, and only the gel in a tube was obtained. As shown in Fig. 4C, the octane interacted with all of the main parts of the nanowires, and the interaction between octane and oleylamine was the strongest. As shown in Fig. 4D, the running diffusion constants of octane, hexane, cyclohexane, and octadecene in the pure state were all higher than the running diffusion constants of them in the gel, respectively, demonstrating that diffusion of organic liquids was limited by nanowire networks (SM materials and methods 3.4) (*17*, *18*). Thus, the good mechanical properties of gels were derived not only from entanglement of nanowires and multilevel interactions between nanowires contributed by electrostatics force and van der Waals force but also by strong interactions between nanowires and organic liquids.

We developed a facile room-temperature synthesis method of AE-POM nanowires. These nanowires could form 3D networks through physical cross-link in the dispersion. Through simply stirring and standing, more than 10 kinds of organic liquids could be locked, such as petrol and octane, and freestanding and elastic organogels were obtained without any additives. On the basis of this method, we easily achieved scalable batch production of nanowires, and kilogram-scale organic liquids could be trapped. Nanowires in gels could be recycled more than 10 times through distillation and centrifugation. And nanowire-based organogels were stable even at liquid-nitrogen temperature. These materials enable semisolidification and spill recovery of organic liquids.

REFERENCES AND NOTES

1. Y. S. Zhang, A. Khademhosseini, *Science* **356**, eaaf3627 (2017).
2. J. A. Burdick, W. L. Murphy, *Nat. Commun.* **3**, 1269 (2012).
3. E. M. Ahmed, *J. Adv. Res.* **6**, 105–121 (2015).
4. S. M. Zhang, X. Wang, *ACS Mater. Lett.* **2**, 639–643 (2020).
5. S. Zhang *et al*., *J. Am. Chem. Soc.* **142**, 1375–1381 (2020).
6. S. Hu, H. Liu, P. Wang, X. Wang, *J. Am. Chem. Soc.* **135**, 11115–11124 (2013).
7. S. M. Zhang *et al*., *Adv. Funct. Mater.* **31**, 2100703 (2021).
8. X. Xu *et al*., *Small* **12**, 2982–2990 (2016).
9. J. E. Boulicault, S. Alves, R. B. Cole, *J. Am. Soc. Mass Spectrom.* **27**, 1301–1313 (2016).
10. R. Rakhshaee, Y. Noorani, *Adv. Powder Technol.* **28**, 1797–1814 (2017).
11. P. Hudec, K. Prandova, *Collect. Czech. Chem. Commun.* **60**, 443–450 (1995).
12. A. Chaumont, G. Wipff, *Phys. Chem. Chem. Phys.* **10**, 6940–6953 (2008).
13. J. M. Maestre, X. Lopez, C. Bo, J. M. Poblet, N. Casañ-Pastor, *J. Am. Chem. Soc.* **123**, 3749–3758 (2001).
14. J. K. Hao, R. A. Weiss, *Polymer* **54**, 2174–2182 (2013).
15. H. H. Hariri, A. M. Lehaf, J. B. Schlenoff, *Macromolecules* **45**, 9364–9372 (2012).
16. V. Normand, D. L. Lootens, E. Amici, K. P. Plucknett, P. Aymard, *Biomacromolecules* **1**, 730–738 (2000).
17. O. Bénichou, P. Illien, G. Oshanin, A. Sarracino, R. Voituriez, *Phys. Rev. Lett.* **115**, 220601 (2015).
18. A. M. Berezhkovskii, L. Dagdug, S. M. Bezrukov, *Biophys. J.* **106**, L09–L11 (2014).

ACKNOWLEDGMENTS

We are grateful for the support of Shuimu Tsinghua Scholar Program and XPLORER PRIZE. **Funding:** This work was supported by the National Natural Science Foundation of China (22035004), the National Key R&D Program of China (2017YFA0700101), and a China Postdoctoral Science Foundation–funded project (2020TQ0164). **Author contributions:** X.W. initiated and guided the research. S.Z. designed and performed the experiments and wrote and revised the manuscript. W.S. performed the simulations. **Competing interests:** The authors declare that they have no competing interests. **Data and materials availability:** All data are available in the main text or the supplementary materials.

SUPPLEMENTARY MATERIALS

science.org/doi/10.1126/science.abm7574
Materials and Methods
Figs. S1 to S28
Tables S1 to S5
References (*19*–*37*)
Movies S1 to S5

Submitted 9 October 2021; resubmitted 11 January 2022
Accepted 1 June 2022
10.1126/science.abm7574

Science

Locking volatile organic molecules by subnanometer inorganic nanowire-based organogels

Simin ZhangWenxiong ShiXun Wang

Science, 377 (6601), • DOI: 10.1126/science.abm7574

Trapping and recovering organics

Hydrogels consist of cross-linked organic polymers that can swell to hold up to 90% water, making them useful as absorbents and for tissue engineering. Zhang *et al*. synthesized inorganic nanowires from polyoxometalates, calcium ions, and oleylamine and found that these nanowires readily formed three-dimensional networks. The networks swell when exposed to a range of volatile organic compounds added at fractions even below 1% to form organogels. The gels are stable to physical squeezing without a substantial loss of liquid. However, the liquids can be recovered using distillation and centrifugation, and the nanowires can be reused, making possible the trapping and recovery of organic solvents. —MSL

Science (ISSN) is published by the American Association for the Advancement of Science. 1200 New York Avenue NW, Washington, DC 20005. The title *Science* is a registered trademark of AAAS.